

Characterization of New Six-Membered Transition States of the Amino-Alcohol Promoted Addition of Dialkyl Zinc to Aldehydes

Torben Rasmussen[†] and Per-Ola Norrby^{*‡}

Department of Medicinal Chemistry
Royal Danish School of Pharmacy, Universitetsparken 2
DK-2100 Copenhagen, Denmark
Department of Organic Chemistry
Technical University of Denmark, Building 201
Kemitorvet, DK-2800 Kgs. Lyngby, Denmark

Received December 1, 2000

The title reaction has been a very popular target for design of chiral ligands ever since 1984, when Oguni and Omi used catalytic amounts of (*S*)-leucinol and obtained moderate enantiomeric excess for the addition of dialkyl zinc to benzaldehyde.¹ Many chiral ligands have since been reported to induce asymmetry in this reaction, the majority of which have been β -amino-alcohols,² but also some featuring other structural motifs.³

Several types of transition states for the title reaction have been proposed in the literature.⁴ Noyori and co-workers have studied the reaction mechanism extensively, both experimentally⁵ and theoretically.⁶ In 1995, Yamakawa and Noyori presented a theoretical investigation of a small model system,^{6a} characterizing two tricyclic transition states — *syn*- and *anti*-orientation of the terminal rings — and one bicyclic TS (Figure 1).

MP2^{6a} and B3LYP⁷ calculations show that the tricyclic *anti*-configuration is the most favored, being 12–13 kJ/mol more stable than the tricyclic *syn*-configuration, and 29 kJ/mol more stable than the bicyclic TS. In the tricyclic transition states, alkyl migration occurs with retention of configuration, whereas the high-energy bicyclic pathway would give inversion of the migrating alkyl group.^{6a}

On the basis of the tricyclic transition states, several selectivity models have been developed.^{6b,8} The major influence of the chiral

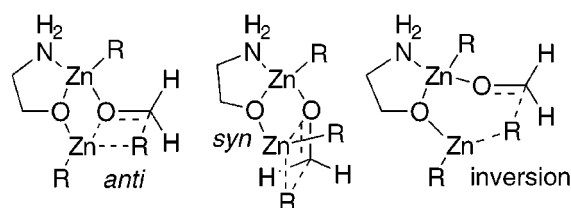


Figure 1. Transition states characterized by Yamakawa and Noyori.⁶

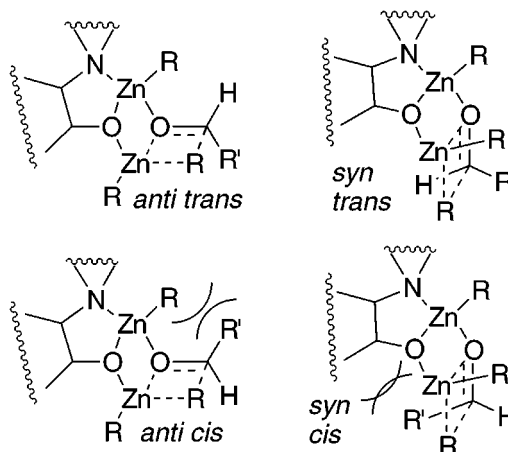
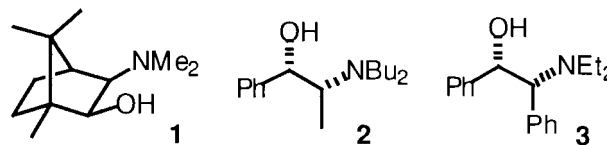


Figure 2. The four major forms of the tricyclic transition state.

ligand is to block one face of the chelated zinc atom. The aldehyde coordinates either lone pair, *cis*, or *trans* to R'. For the favored zinc face, the four possible tricyclic transition states are shown in Figure 2. The most favorable of these configurations is usually *anti-trans*.⁹ The minor enantiomer can arise via the *syn-trans* or *anti-cis* pathways, whereas *syn-cis* (leading to the same product as *anti-trans*) is highly disfavored due to steric crowding.

We have implemented a Q2MM¹⁰ force field for the title reaction to allow rapid evaluation of new ligands. In line with previous work in our group¹¹ we had expected an accuracy around 2 kJ/mol for enantioselectivity predictions from the force field. Testing against a set of known ligands with diverse selectivity revealed that many systems (e.g., DAIB, **1**) were predicted within the target accuracy, but some prominent outliers were identified, among them the DBNE ligand (**2**).⁹ No obvious parameter deficiencies could be identified, and inclusion of additional data points in the parametrization did not change the picture significantly. Goldfuss and Houk have shown that the behavior of the very similar ligand **3** could be rationalized by PM3,^{8b} and we therefore subjected our best conformations of **2** to optimization using this unbiased method.¹²



Surprisingly, a new low-energy path was identified when attempting to locate an *anti-cis* transition state. The new mechanism

- (8) (a) Vidal-Ferran, A.; Moyano, A.; Pericàs, M. A.; Riera, A. *Tetrahedron Lett.* **1997**, *38*, 8773–8776. (b) Goldfuss, B.; Houk, K. N. *J. Org. Chem.* **1998**, *63*, 8998–9006. (c) Goldfuss, B.; Steigelmann, M.; Khan, S. I.; Houk, K. N. *J. Org. Chem.* **2000**, *65*, 77–82. (d) Vázquez, J.; Pericàs, M. A.; Maseras, F.; Lledós, A. *J. Org. Chem.* **2000**, *65*, 7303–7309. (e) Goldfuss, B.; Steigelmann, M.; Rominger, F. *Eur. J. Org. Chem.* **2000**, 1785–1792.
(9) Rasmussen, T. Manuscript in preparation.
(10) Q2MM; transition-state MM force field based on specific types of QM data: Norrby, P.-O. *J. Mol. Struct. (THEOCHEM)* **2000**, *506*, 9–16.

[†] Royal Danish School of Pharmacy.

[‡] Technical University of Denmark, okpon@pop.dtu.dk.

(1) Oguni, N.; Omi, T. *Tetrahedron Lett.* **1984**, *25*, 2823–2824.

(2) (a) Cho, B. T.; Chun, Y. S. *Tetrahedron: Asymmetry* **1998**, *9*, 1489–1492. (b) Guijarro, D.; Pinho, P.; Andersson, P. G. *J. Org. Chem.* **1998**, *63*, 2530–2535. (c) Shi, M.; Satoh, Y.; Masaki, Y. *J. Chem. Soc., Perkin Trans. I* **1998**, 2547–2552. (d) Tanner, D.; Kornø, H. T.; Guijarro, D.; Andersson, P. G. *Tetrahedron* **1998**, *54*, 14213–14232. (e) Kossenjans, M.; Soeberdt, M.; Wallbaum, S.; Harms, K.; Martens, J.; Aurich, H. G. *J. Chem. Soc., Perkin Trans. I* **1999**, 2353–2365. (f) Lawrence, C. F.; Nayak, S. K.; Thijs, L.; Zwanenburg, B. *Synlett* **1999**, *10*, 1571–1572. (g) Sibi, M. P.; Chen, J.-x.; Cook, G. R. *Tetrahedron Lett.* **1999**, *40*, 3301–3304. (h) Wassmann, S.; Wilken, J.; Martens, J. *Tetrahedron: Asymmetry* **1999**, *10*, 4437–4445. (i) Yang, X.; Shen, J.; Da, C.; Wang, R.; Choi, M. C. K.; Yang, L.; Wong, K. *Tetrahedron: Asymmetry* **1999**, *10*, 133–138. (j) Kawanami, Y.; Mitsuie, T.; Miki, M.; Sakamoto, T.; Nishitani, K. *Tetrahedron* **2000**, *56*, 175–178. (k) Reddy, K. S.; Solà, L.; Moyano, A.; Pericàs, M. A.; Riera, A. *Synthesis* **2000**, *1*, 165–176.

(3) (a) Gibson, C. L. *Tetrahedron: Asymmetry* **1999**, *10*, 1551–1561. (b) Chuang, T.-H.; Fang, J.-M.; Bolm, C. *Synth. Commun.* **2000**, *30*, 1627–1641. (c) Dangel, B. D.; Polt, R. *Org. Lett.* **2000**, *2*, 3003–3006.

(4) (a) Itsuno, S.; Fréchet, J. M. J. *J. Org. Chem.* **1987**, *52*, 4140–4142. (b) Evans, D. A. *Science* **1988**, *240*, 420–426. (c) Corey, E. J.; Yuen, P.-W.; Hannon, F. J.; Wierda, D. A. *J. Org. Chem.* **1990**, *55*, 784–786. (d) Noyori, R.; Kitamura, M. *Angew. Chem., Int. Ed. Engl.* **1991**, *30*, 49–69.

(5) (a) Kitamura, M.; Okada, S.; Suga, S.; Noyori, R. *J. Am. Chem. Soc.* **1989**, *111*, 4028–4036. (b) Kitamura, M.; Oka, H.; Noyori, R. *Tetrahedron* **1999**, *55*, 3605–3614.

(6) (a) Yamakawa, M.; Noyori, R. *J. Am. Chem. Soc.* **1995**, *117*, 6327–6335. (b) Yamakawa, M.; Noyori, R. *Organometallics* **1999**, *18*, 128–133.

(7) Current work. All geometry optimizations were performed at the B3LYP/LACVP* level (double- ζ valence + ECP for Zn, 6-31G* for others) in Jaguar 4.0 from Schrödinger Inc., <http://www.schrodinger.com>. Transition states were verified by normal-mode analysis. Selected single-point calculations were performed using the triple- ζ valence LACV3P++** basis, or the PB-SCRF solvation model.

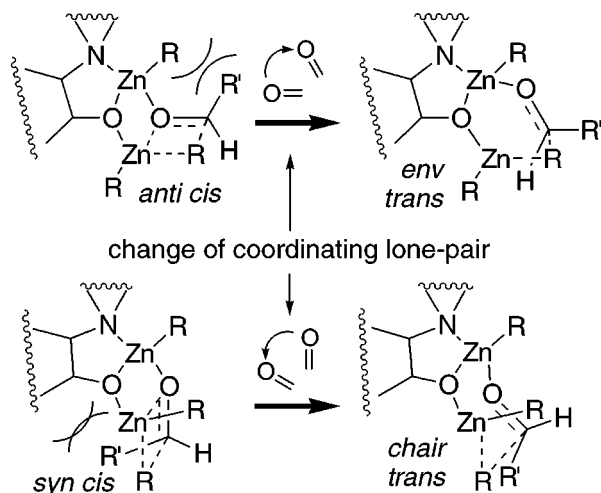


Figure 3. Comparison between the previous and new mechanisms.

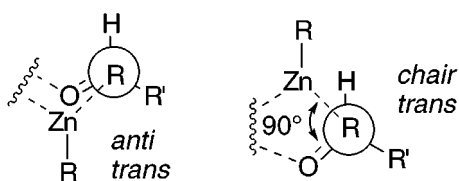


Figure 4. Newman-type projection of the forming C-C bond.

is formally related to the old by a change in the coordinating lone-pair on the carbonyl oxygen, (e.g., *cis* \rightarrow *trans*, Figure 3). To retain best possible overlap with the migrating alkyl group, the structure opens to a bicyclic configuration, including a six-membered ring with an envelope (*env*) conformation. In all previously proposed mechanisms the two breaking bonds (zinc-alkyl and carbonyl) are close to parallel,⁸ whereas in the new TS the bonds are almost perpendicular (Figure 4). In contrast to the high-energy six-membered TS reported earlier (Figure 1), the new six-membered transition states give migration with retention of configuration, just like the tricyclic ones. A *chair* TS arises formally from the *syn-cis* TS in a similar manner. For **2**, the new transition states, *env* and *chair*, are lower in energy than the best *anti* form by 19 and 50 kJ/mol, respectively. The lowest form, *chair-trans*, does indeed lead to the observed major enantiomer.

A small-model system constructed from dimethylamino ethanol, dimethyl zinc, and formaldehyde was investigated using DFT.⁷ Similar to the results of Noyori and co-workers,⁶ the *anti* TS was lowest in energy, with the *syn* TS 13 kJ/mol higher. The two new transition states (*env* and *chair*) were located 16 kJ/mol above the *anti* TS (Figure 5). Employing a continuum solvation model, *env* is 13 kJ/mol above *anti* in toluene and only 11 kJ/mol higher in THF, slightly lower than *syn*. At the triple- ζ level in the gas phase, *env* is only 9 kJ/mol above *anti*.

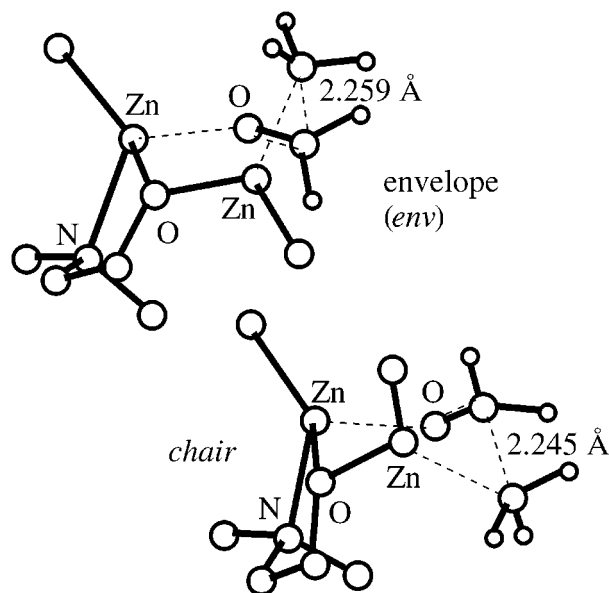


Figure 5. New six-membered transition states, *env* and *chair*. Innocent hydrogens are hidden for clarity.

At the PM3 level, the formaldehyde model could not be converged to the *anti* or *syn* TS. Employing instead a *trans*-acetaldehyde model, PM3 identified *env* as the lowest path, 31 kJ/mol below *anti*, whereas DFT shows *anti* to be 18 kJ/mol lower than *env* in the gas phase (a shift by 2 kJ/mol from the formaldehyde model). This discrepancy must be considered when using PM3 to calculate transition states for larger systems, but considering all error sources it is still likely that the favored TS for **2** is the *chair* form. A final resolution of this question will have to await evaluation of the transition states for **2** by a more accurate method such as QM/MM.^{8c-e}

The results illustrate some of the relative merits of different methods for assessing reaction selectivities. The Q2MM method, by virtue of allowing full searching of the conformational space, can pinpoint cases where the tricyclic transition-state model fails to rationalize the observed selectivity, but only QM or QM/MM can show the reason for the failure. Thus, the techniques are complementary: the Q2MM method allows rapid scanning and sometimes accurate predictions, whereas the slower QM-based methods can reproduce changes in the reaction coordinate.

The successful rationalization of experimental data using the old transition states indicate that for many systems the tricyclic transition states are favored.^{8,9} However, it is clear from the current results that the new transition states could constitute the dominant path to the minor enantiomer in solvent, and for some substrates could also be the major source of both enantiomers. Thus, future design and rationalization of the title reaction should consider the alternative paths described herein.

Acknowledgment. Support from the Danish Technical Research Council is gratefully acknowledged.

Supporting Information Available: Geometries and energies of B3LYP and PM3 transition states (PDF). This material is available free of charge via the Internet at <http://pubs.acs.org>.

JA005841K

(11) (a) Norrby, P.-O. In *Transition State Modeling for Catalysis*; Truhlar, D. G., Morokuma, K., Eds.; ACS Symposium Series 721; American Chemical Society: Washington, DC, 1999; pp 163–172. (b) Norrby, P.-O.; Brandt, P.; Rein, T. *J. Org. Chem.* **1999**, *64*, 5845–5852. (c) Norrby, P.-O.; Rasmussen, T.; Haller, J.; Strassner, T.; Houk, K. N. *J. Am. Chem. Soc.* **1999**, *121*, 10186–10192.

(12) PM3 calculations were performed using the MOPAC97 module in Chem3D from CambridgeSoft, <http://www.camsoft.com>.